AD-A129 866 RESONANCE FLUORESCENCE OF MANY INTERACTING ADATOMS AT A METAL SURFACE(U) ROCHESTER UNIV NY DEPT OF CHEMISTRY X HUANG ET AL. JUN 83 UROCHESTER/DC/83/TR-34 1/1

UNCLASSIFIED N00014-80-C-0472 F/G 7/4 NL

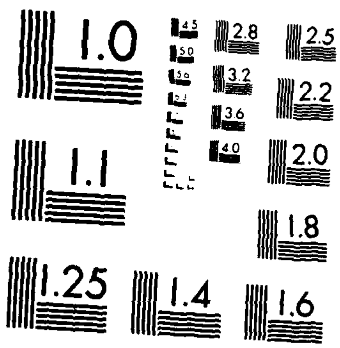

MICROCOPY RESOLUTION TEST CHART
NATIONAL BUREAU OF STANDARDS-1963-A

ADA129866

OFFICE OF NAVAL RESEARCH

Contract N00014-80-C-0472

Task No. NR 056-749

TECHNICAL REPORT No. 34

Resonance Fluorescence of Many
Interacting Adatoms at a Metal Surface

by

Xi-Yi Huang, Thomas F. George and Jui-teng Lin

Prepared for Publication

in

Coherence and Quantum Optics V,
Proceedings of the Fifth Rochester Conference on Coherence
and Quantum Optics, ed. by L. Mandel and E. Wolf (Plenum, New York)

Department of Chemistry
University of Rochester
Rochester, New York 14627

DTIC FILE COPY

DTIC

June 1983

Reproduction in whole or in part is permitted for any
purpose of the United States Government.

This document has been approved for public release
and sale; its distribution is unlimited.

Unclassified

SECURITY CLASSIFICATION OF THIS PAGE (When Data Entered)

REPORT DOCUMENTATION PAGE		READ INSTRUCTIONS BEFORE COMPLETING FORM
1. REPORT NUMBER UROCHESTER/DC/83/TR-34	2. GOVT ACCESSION NO. AD-A129 266	3. RECIPIENT'S CATALOG NUMBER
4. TITLE (and Subtitle) Resonance Fluorescence of Many Interacting Adatoms at a Metal Surface		5. TYPE OF REPORT & PERIOD COVERED 6. PERFORMING ORG. REPORT NUMBER
7. AUTHOR(s) Xi-Yi Huang, Thomas F. George and Jui-teng Lin		8. CONTRACT OR GRANT NUMBER(s) N00014-80-C-0472
9. PERFORMING ORGANIZATION NAME AND ADDRESS Department of Chemistry University of Rochester Rochester, New York 14627		10. PROGRAM ELEMENT, PROJECT, TASK AREA & WORK UNIT NUMBERS NR 056-749
11. CONTROLLING OFFICE NAME AND ADDRESS Office of Naval Research Chemistry Program Code 472 Arlington, Virginia 22217		12. REPORT DATE June 1983 13. NUMBER OF PAGES 10
14. MONITORING AGENCY NAME & ADDRESS(if different from Controlling Office)		15. SECURITY CLASS. (of this report) Unclassified 15a. DECLASSIFICATION/DOWNGRADING SCHEDULE

16. DISTRIBUTION STATEMENT (of this Report)

This document has been approved for public release and sale; its distribution is unlimited.

17. DISTRIBUTION STATEMENT (of the abstract entered in Block 20, if different from Report)

18. SUPPLEMENTARY NOTES

Prepared for publication in Coherence and Quantum Optics V, Proceedings of the Fifth Rochester Conference on Coherence and Quantum Optics, ed. by L. Mandel and E. Wolf (Plenum, New York)

19. KEY WORDS (Continue on reverse side if necessary and identify by block number)

RESONANCE FLUORESCENCE	POWER SPECTRUM
TWO-LEVEL ATOM	SURFACE DRESSED BLOCH EQUATIONS
METAL SURFACE	MANY ADATOMS
REFLECTED FIELD	MIGRATION EFFECTS
POPULATION INVERSION	PHONON-INDUCED LEVEL BROADENING

20. ABSTRACT (Continue on reverse side if necessary and identify by block number) A model of resonance fluorescence of a laser-driven two-level atom near a metal surface is reviewed, and results are shown in the weak-field limit for the population inversion and the power spectrum. Extension of the model to interacting adatoms is discussed in terms of phonon-induced level broadening and adatom migration.

To appear in the *Proceedings of the Fifth Rochester Conference on Coherence and Quantum Optics*, ed. by L. Mandel and E. Wolf (Plenum, New York).

RESONANCE FLUORESCENCE OF MANY INTERACTING ADATOMS AT A METAL SURFACE

Xi-Yi Huang and Thomas F. George

Department of Chemistry
University of Rochester
Rochester, New York 14627

and

Jui-teng Lin

Laser Physics Branch
Optical Sciences Division
Naval Research Laboratory
Washington, D.C. 20375

ABSTRACT

A model of resonance fluorescence of a laser-driven two-level atom near a metal surface is reviewed, and results are shown in the weak-field limit for the population inversion and the power spectrum. Extension of the model to interacting adatoms is discussed in terms of phonon-induced level broadening and adatom migration.

INTRODUCTION

Recently there has been considerable theoretical and experimental interest in the interaction of electromagnetic radiation with surfaces. The perfection of the fatty-acid monolayer assembly technique has led to a series of experiments in which the fluorescence of an excited atom or molecule at a fixed distance from a metal surface (gold, silver and cooper) was measured.[1] Experiments have also demonstrated enhanced luminescence and resonance fluorescence for adspecies on metals (and also on dielectric fibers) as compared to the surface-free molecules.[2,3] In order to understand the excitation-relaxation behavior and resonance fluorescence spectrum of a laser-driven atom near a metal surface, we choose in this paper a simple two-level model for the adatom, combined with the techniques of quantum optics. We shall first review the model for a single adatom and then extend it to many interacting adatoms.

SINGLE TWO-LEVEL ADATOM

We assume the adatom to be driven by a partially-coherent laser field. Although the atom has no dipole moment in its ground state, it can have a significant induced transition dipole in a driving field. The reflected field provided by a metallic mirror and surface plasmon resonance can influence the dynamic behavior and light scattering spectrum of the adatom. The field reflected by the metallic surface takes the quantum form[4]

$$E_R(t) = \mu_{12}\sigma_{12}(t)\, f(d) + \mu_{21}\sigma_{21}(t)\, f^*(d), \tag{1}$$

where μ_{ij} is the transition dipole between adatomic states $|i\rangle$ and $|j\rangle$, $\sigma_{ij} \equiv |i\rangle\langle j|$ is the adatomic transition operator, and $f(d)$ is a frequency-dependent and adatom-metal distance-dependent (d) function which will be discussed in more detail later.

In the rotating-wave approximation (RWA), the surface-dressed optical Bloch equations (SBE) can be written (assuming the equilibrium condition $\hat{W} = -1$)

$$\frac{d}{dt}\begin{pmatrix}\hat{S}_{21}(t)\\ \hat{W}(t)\\ \hat{S}_{12}(t)\end{pmatrix} = \begin{pmatrix}-\tilde{\gamma}_2 + i\Delta & i\Omega^-(t)/2 & 0\\ i\Omega^+(t) & -\gamma_1 & -i\Omega^-(t)\\ 0 & -i\Omega^+(t)/2 & -\tilde{\gamma}_2 - i\Delta\end{pmatrix}\begin{pmatrix}\hat{S}_{21}(t)\\ \hat{W}(t)\\ \hat{S}_{12}(t)\end{pmatrix}$$

$$-\gamma_1\begin{pmatrix}0\\1\\0\end{pmatrix}. \tag{2}$$

$\hat{W}(t)$ is the population inversion; $\hat{S}_{21}(t) \equiv \hat{\sigma}_{21}(t)\exp(-i\omega_L(t)$; $\Omega^{\pm} \equiv \Omega\exp[\mp i\phi)t)]$, where $\Omega \equiv 2|\mu_{21}|E_o(t)/\hbar$ is the regular Rabi frequency and the electric field $E(t)$ of laser is written in terms of the amplitude $E_o(t)$ and phase factor ϕ as $E_o(t)\exp(-i\omega_L t - i\phi(t)) + c.c.$; $\Delta \equiv \omega_{21} - \omega_L$ is the detuning, where ω_{21} is the transition frequency of the adatom and ω_L is the laser frequency; the surface-induced phase-decay constant is $\gamma_s \equiv 2\,\mathrm{Im}(f)|\mu_{12}|^2/\hbar$; $\tilde{\gamma}_2 \equiv \gamma_2 + \gamma_s$; γ_1 and γ_2 are the population and phase decay constant, respectively, in the surface-free case. We have implicitly included the interatomic collision effects by letting $\gamma_1 \neq 2\gamma_2$.

To calculate γ_s, we must know the complex function $f(d)$, which can be determined by the Sommerfeld-Hertz vector procedure,[5]

$$\mathrm{Im}(f) = \frac{\zeta}{1+\epsilon_1^2} \frac{k_1^3}{(\omega^2 - \omega_{sp}) + \frac{\delta^2\omega_{sp}^4}{\omega^2}}$$

$$\{\frac{1}{\epsilon_1}[(\omega^2-\omega_p^2)^2 + \frac{\omega_p^4\delta^2}{\omega^2} - \epsilon_1^2\omega^4][\eta \sin D - \frac{1}{D^2}\cos D]$$

$$+ 2\omega\delta\omega_p^2[\eta \cos D + \frac{1}{D^2}\sin D]\} , \qquad (3)$$

where $\zeta = 1$ and $\eta \equiv \frac{1}{D^3} + \frac{1}{D}$ for the case of the induced dipole oriented parallel to the surface, $\zeta = 2$ and $\eta \equiv \frac{1}{D^2}$ for the perpendicular case, ϵ_1 is the dielectric constant for the gas medium, $k_1 = \omega\sqrt{\epsilon_1}/c$ is the wave number, ω is the emission frequency, and $D = 2k_1 d$ is the reduced distance which is dimensionless. The Drude model $\epsilon_2(\omega) = 1 - \frac{\omega_p^2}{\omega(\omega+i\delta)}$ has been utilized, where δ is the inverse of the relaxation time, ω_p is the plasma frequency, and $\omega_{sp} = \omega_p(1+\epsilon_1)^{-1/2}$ is the surface plasmon frequency of the interface.

Equation (3) leads to a surface-induced phase-decay constant γ_s (in the unit of Einstein's spontaneous decay constant A) of the following form:

$$\gamma_s = \zeta a_o[a_1(\eta \sin D - \frac{\cos D}{D^2}) + a_2(\eta \cos D + \frac{\sin D}{D^2})], \qquad (4)$$

where $a_o \equiv 3/8[(1-\beta^2)^2 + (\alpha/\omega_{sp})^2]$, $a_1 = (2-\beta^2)^2 + (2\alpha/\omega_{sp})^2 - \beta^4$, $a_2 = (2\beta)^2\alpha/\omega_{sp}$, and $\beta \equiv \omega_L/\omega_{sp}$, $\alpha \equiv \delta/\beta$ and $\epsilon_1 = 1$ has been assumed. The above expression for γ_s can be further simplified by assuming perfect reflection, i.e., $R^\perp = R^\parallel = -1$, where $R^\perp$ ($R^\parallel$) is the reflection coefficient for an incident ray polarized perpendicular (parallel) to the plane of incidence. Then

$$\gamma_s = \frac{3}{2}\zeta(\eta \sin D - \frac{\cos D}{D^2}). \qquad (5)$$

We use the phase-diffusion model[6] for the laser field: $\langle\langle\Omega^-(t_1)\Omega^+(t_2)\rangle\rangle = \Omega^2 \exp(-\gamma_L|t_2-t_1|)$, where γ_L is the laser bandwidth. We consider the weak-field or large-detuning limit, wherein $W(t) = \langle\langle\hat{W}(t)\rangle\rangle \approx -1$. The double bracket signifies an average over the stochastic ensemble and a quantum mechanical average. Assuming the laser field to be turned on at $t = 0$ with a constant amplitude for $t \geqslant 0$, we can obtain an analytical form for the population inversion.[4] The power spectrum $S(\omega)$ as a function of the emission frequency ω is given by the Fourier transform of the dipole-dipole correlation function, and for steady state it can also be obtained analytically to yield the expression[4]

$$S(\omega) = \frac{\Omega^2}{2}\frac{1}{(\tilde{\gamma}_2+\gamma_L)^2+\Delta^2}\{\frac{1}{(\tilde{\gamma}_2-\gamma_L)^2+\Delta^2}[\frac{\gamma_L(\tilde{\gamma}_2^2-\gamma_L^2+\Delta^2) + 2\gamma_L\Delta(\omega-\omega_L)}{\gamma_L^2 + (\omega-\omega_L)^2}$$

$$-\frac{\tilde{\gamma}_2(\tilde{\gamma}_2^2-\gamma_L^2+\Delta^2) + 2\gamma_L\Delta(\omega-\omega_{21})}{\tilde{\gamma}_2^2 + (\omega-\omega_{21})^2}] + \frac{2(\tilde{\gamma}_2+\gamma_L)\tilde{\gamma}_2}{\gamma_1[\tilde{\gamma}_2^2 + (\omega-\omega_{21})^2]}\}. \tag{6}$$

Sample results for these analytical forms of $W(t)$ and $S(\omega)$ are shown in Figure 1. The time evolution of $W(t)$ is shown in the upper part of the figure for two different adatom-surface plasmon resonance conditions: $\beta = 0.5$ and $\beta = 0.9$. We have used the value of 3.5×10^{-3} for the ratio δ/ω_{sp}, which corresponds to a silver surface. We make the following three observations: (i) Each curve approaches a stationary-state value for large t. (ii) The value of W depends on the adatom-surface plasmon resonance condition β and the reduced adatom-surface distance D. Generally, the values of W for the off-resonance case ($\beta = 0.5$) are less than those for the near-resonance case ($\beta = 0.9$). Furthermore, the values of W for larger D are less than those for smaller D, since the levels of the adatom for smaller D are strongly broadened by the adatom-surface interaction, so that the population of the upper level increases. (iii) For large D (curve 3), the curves for $\beta = 0.5$ and $\beta = 0.9$ coincide, since the adatom-surface coupling tends to vanish. The strong oscillations in this nearly surface-free situation are caused by beating between the driving laser field and the "adatomic oscillator".

The bottom part of Figure 1 displays the resonance fluorescence power spectrum, with the Rayleigh peak near $\omega = \omega_L$ and fluorescence peak near $\omega = \omega_{21}$. The latter peak is strongly dependent on D and β. As D decreases and β approaches unity, the upper adatomic level broadens, and hence the power in the fluorescence peak increases.

MANY ADATOMS

So far we have studied the SBE and resonance fluorescence for a single-adatom system in which the main effects of the surface are characterized by the reflected field and the adatom-plasmon inter-

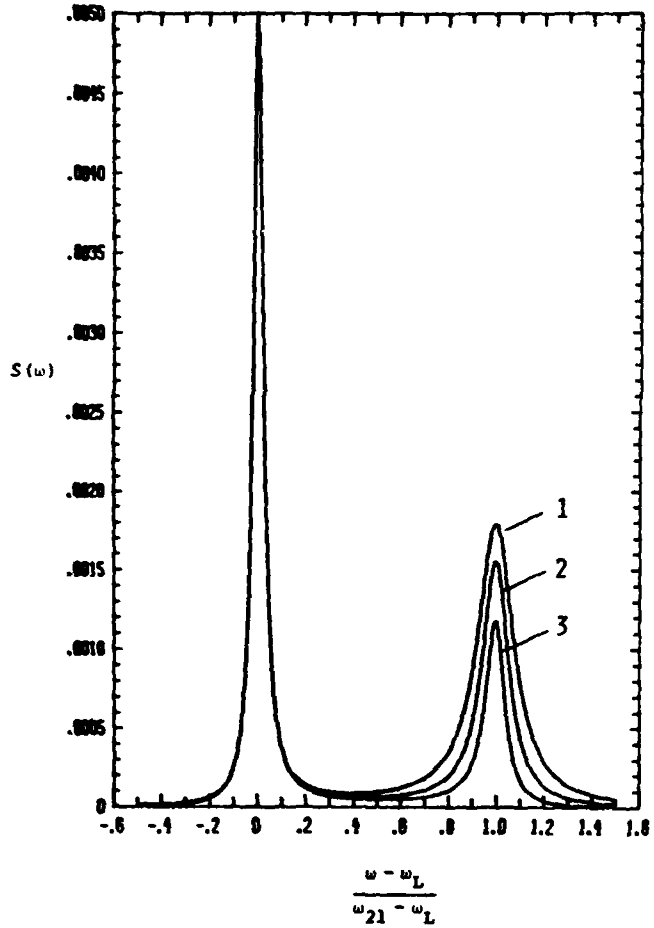

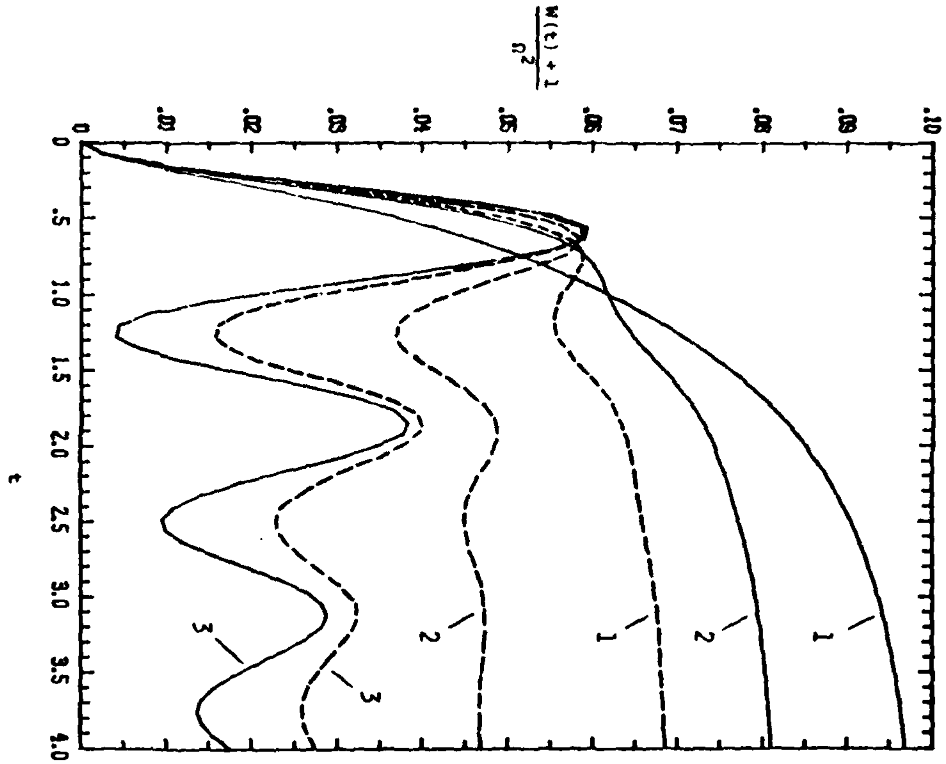

Figure 1. Population inversion (upper part) and resonance fluorescence power spectrum (lower part) in the weak-field or large-detuning limit, with $(\gamma_L, \Omega, \Delta) = (0.3, 0.05, 5)$ in the unit A for $\beta=0.9$ (solid curves) and $\beta=0.5$ (dashed curves). The induced transition dipole is oriented perpendicular to the surface. Curves 1, 2 and 3 correspond to $D = 2k_1d = 1$, 3 and 5, respectively. The time axis is in the unit A^{-1}, and the units for $S(\omega)$ are arbitrary.

action. For a system consisting of many adatoms as depicted in Figure 2, the SBE may be derived by taking an ensemble average over the adatoms. We note that the cooperative feature of a many-adatom system can be significantly different from that of the single-adatom system due to static processes, such as dipole-dipole coupling, and dynamical processes, such as collisional broadening among the mobile adatoms. We also note that the adatoms together with the surface atoms may actually form a "pseudomolecule" whose vibrational degrees of freedom may be coupled to the electronic excitations. To describe the many-body features of the system, one can write a total Hamiltonian as

$$H = H_A + H_B + H_{AB} + H_{AA} + H_{ABA} + H_{AR} + H_{BB} + H_{AF}. \tag{7}$$

H_A and H_B are the unperturbed Hamiltonians for the adatoms (A) and the phonon bath modes (B), respectively, with a coupling interaction H_{AB}; H_{AA} and H_{ABA} represent the adatom-adatom interactions via direct dipole-dipole coupling or phonon-mediated coupling; H_{AR} represents the interaction between the adatoms and reflected field and/or surface plasmon; H_{BB} describes energy diffusion on and into the substrate via phonon-phonon coupling; and

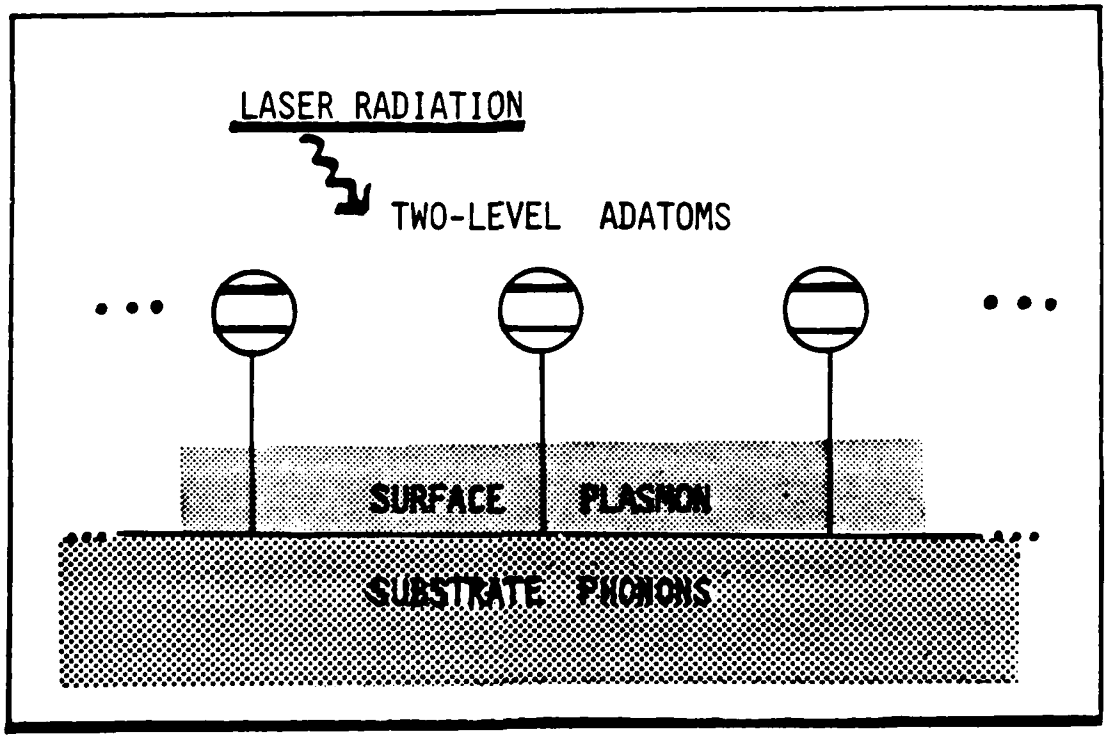

Figure 2. Schematic diagram for a many-adatom system in which two-level adatoms are excited by laser radiation and coupled to the surface plasmon and substrate phonons as described by the total Hamiltonian of Equation (7).

H_{AF} is the radiative coupling between the applied laser field and the adatoms. To derive the SBE, a second-quantized form of the above Hamiltoniam, involving dipole operators for the adatoms and harmonic operators for the phonon modes, is appropriate. The mathematical form may be found in References 7 and 8 and is not shown here. Instead, we want to discuss below the physical mechanisms associated with the individual terms of the total Hamiltonian.

From the SBE we see that the overall level broadening of an adatom is characterized by phase relaxation (Γ_2) and energy relaxation (Γ_1). The relaxation factors may be decomposed as

$$\Gamma_1 = \gamma_1 + \gamma_{1B} + \gamma_{1R} \tag{8}$$

$$\Gamma_2 = \tilde{\gamma}_2 + \gamma_{2B} + \gamma_{2R} \; . \tag{9}$$

γ_1 and $\tilde{\gamma}_2$ are the previously-defined relaxation factors or decay constants for a single-adatom system except that the collision-induced broadening in $\tilde{\gamma}_2$ is modified further by the migration of the adatoms. γ_{1B} and γ_{2B} are the relaxation factors due to electron-phonon coupling, and γ_{1R} and γ_{2R} are due to the reflected field. Depending on the interaction mechanisms, these phase and energy relaxation factors are influenced differently by the system's parameters such as the adatom-surface distance, the coverage or the adatom-adatom distance, the surface temperature and the frequency spectra of the whole system. Some of the important features are the following:

(i) The phonon-induced broadening γ_B resulting from H_{AB} and H_{BB} is strongly temperature dependent through the phonon occupation number and is governed by the frequency spectra of the phonon modes.[8] For example, for an adatom with frequency closer to the Debye frequency, we expect a stronger coupling, or larger γ_B.

(ii) The dephasing broadening $\tilde{\gamma}_2$ due to the adatom-plasmon interaction may be further broadened via H_{AA} and H_{ABA} in which the collisional effects may be significant for a high-coverage system and/or highly mobile adatoms in physisorbed states.

(iii) The reflected-field broadening γ_{1R} is related to Re(f) and γ_{2R} to Im(f) due to H_{AR}. The direct (H_{AA}) and phonon-mediated (H_{ABA}) adatom-adatom interactions through their near dipole field and exchange of photons are slowly-varying functions of their separations compared with the dependence of those effects due to H_{AR} on the reduced distance.[10]

We finally note that the influence of the surface on the SBE and the resonance fluorescence is exhibited through the level broadenings characterized by the above relaxation factors $\Gamma_{1,2}$ and the adatomic frequency shift. To include the effects of the frequency shift, the detuning Δ defined earlier should be replaced be an effective detuning $\tilde{\Delta}$. The effective resonance condition $\tilde{\Delta} = 0$ may be met by means of the continuum phonon spectra. Furthermore, when a two-level adatom moves close to the surface to form a bond, e.g., physisorbed to the substrate, it becomes a multilevel system in which each electronic level has many vibrational sublevels.

SUMMARY

A model has been developed to describe the dynamical behavior of a two-level adatom at a metal surface. Surface-dressed optical Bloch equations (SBE), which account for surface-reflected photons and adatom-surface plasmon coupling, have been derived. Collisions with foreign gas atoms and effects of the laser bandwidth have been included. The population inversion and the power spectrum of the scattered light for a single adatom have been evaluated. These quantities exhibit behavior which is strongly dependent on the adatom surface distance and adatom-surface plasmon resonance. For a many-adatom system, the SBE and the resonance fluorescence are influenced not only by static interactions, such as dipole-dipole coupling, electron-phonon coupling and the phonon-mediated adatom-adatom interactions, but also by dynamical type processes, such as laser-enhanced migration of the adatoms.

ACKNOWLEDGEMENTS

This work was supported in part by the Air Force Office of Scientific Research (AFSC) under Grant No. AFOSR-82-0046, the U.S. Army Research Office and the Office of Naval Research. The United States Government is authorized to reproduce and distribute reprints for governmental purposes notwithstanding any copyright notation hereon. TFG acknowledges the Camille and Henry Dreyfus Foundation for a Teacher-Scholar Award (1975-84) and the John Simon Guggenheim Memorial Foundation for a Fellowship (1983-84).

REFERENCES

1. K. H. Drexhage, Interaction of Light with Monomolecular Dye Layers, in "Progress in Optics XII," E. Wolf, ed., North-Holland, Amsterdam (1974), p. 165.
2. A. M. Glass, P. F. Liao, J. C. Bergman and D. H. Olson, Interaction of Metal Particles with Adsorbed Dye Molecules: Absorption and Luminescence, Opt. Lett. 5: 368 (1968).
3. J. F. Owen, P. W. Barber, P. B. Dorain and R. K. Chang, Enhancement of Fluorescence Induced by Microstructure Resonances of a Dielectric Fiber, Phys. Rev. Lett. 47: 1075 (1981).

4. X. Y. Huang, T. F. George and J. Lin, Resonance Fluorescence of a Two-Level Atom Near a Metal Surface, J. Chem. Phys., in press.
5. See the review by R. R. Chance, A. Prock and R. Silbey, Molecular Fluorescence and Energy Transfer Near Interfaces, Adv. Chem. Phys. 37: 1 (1978).
6. J. H. Eberly, Atomic Relaxation in the Presence of Intense Partially Coherent Radiation Feilds, Phys. Rev. Lett. 37: 1387 (1976).
7. J. Lin, X. Y. Huang and T. F. George, Quantum Dynamical Model for Laser Excitation of a Two-Level Adatom: Surface-Dressed Bloch Equations, Solid State Commun. 47: 63 (1983).
8. J. Lin and T. F. George, Dynamical Model of Selective vs. Nonselective Laser-Stimulated Surface Processes. 2. Analytical Methods and Applications to Surface Rate Processes, J. Phys. Chem. 84: 2957 (1980).
9. M. Kús and K. Wódkiewicz, Two-Atom Resonance Fluorescence, Phys. Rev. 23: 853 (1981).
10. M. J. Stephen, First-Order Dispersion Forces, J. Chem. Phys. 40: 669 (1964).

TECHNICAL REPORT DISTRIBUTION LIST, GEN

	No. Copies
Office of Naval Research Attn: Code 413 800 North Quincy Street Arlington, Virginia 22217	2
ONR Pasadena Detachment Attn: Dr. R. J. Marcus 1030 East Green Street Pasadena, California 91106	1
Commander, Naval Air Systems Command Attn: Code 310C (H. Rosenwasser) Department of the Navy Washington, D.C. 20360	1
Defense Technical Information Center Building 5, Cameron Station Alexandria, Virginia 22314	12
Dr. Fred Saalfeld Chemistry Division, Code 6100 Naval Research Laboratory Washington, D.C. 20375	1
U.S. Army Research Office Attn: CRD-AA-IP P. O. Box 12211 Research Triangle Park, N.C. 27709	1
Mr. Vincent Schaper DTNSRDC Code 2803 Annapolis, Maryland 21402	1
Naval Ocean Systems Center Attn: Dr. S. Yamamoto Marine Sciences Division San Diego, California 91232	1
Dr. David L. Nelson Chemistry Program Office of Naval Research 800 North Quincy Street Arlington, Virginia 22217	1
Naval Ocean Systems Center Attn: Mr. Joe McCartney San Diego, California 92152	1
Naval Weapons Center Attn: Dr. A. B. Amster, Chemistry Division China Lake, California 93555	1
Naval Civil Engineering Laboratory Attn: Dr. R. W. Drisko Port Hueneme, California 93401	1
Dean William Tolles Naval Postgraduate School Monterey, California 93940	1
Scientific Advisor Commandant of the Marine Corps (Code RD-1) Washington, D.C. 20380	1
Naval Ship Research and Development Center Attn: Dr. G. Bosmajian, Applied Chemistry Division Annapolis, Maryland 21401	1
Mr. John Boyle Materials Branch Naval Ship Engineering Center Philadelphia, Pennsylvania 19112	1
Mr. A. M. Anzalone Administrative Librarian PLASTEC/ARRADCOM Bldg 3401 Dover, New Jersey 07801	1

TECHNICAL REPORT DISTRIBUTION LIST, 056

	No. Copies
Dr. G. A. Somorjai Department of Chemistry University of California Berkeley, California 94720	1
Dr. J. Murday Naval Research Laboratory Surface Chemistry Division (6170) 455 Overlook Avenue, S.W. Washington, D.C. 20375	1
Dr. J. B. Hudson Materials Division Rensselaer Polytechnic Institute Troy, New York 12181	1
Dr. Theodore E. Madey Surface Chemistry Section Department of Commerce National Bureau of Standards Washington, D.C. 20234	1
Dr. J. M. White Department of Chemistry University of Texas Austin, Texas 78712	1
Dr. Keith H. Johnson Department of Metallurgy and Materials Science Massachusetts Institute of Technology Cambridge, Massachusetts 02139	1
Dr. J. E. Demuth IBM Corporation Thomas J. Watson Research Center P. O. Box 218 Yorktown Heights, New York 10598	1
Dr. C. P. Flynn Department of Physics University of Illinois Urbana, Illinois 61801	1

	No. Copies
Dr. W. Kohn Department of Physics University of California (San Diego) La Jolla, California 92037	1
Dr. R. L. Park Director, Center of Materials Research University of Maryland College Park, Maryland 20742	1
Dr. W. T. Peria Electrical Engineering Department University of Minnesota Minneapolis, Minnesota 55455	1
Dr. Chia-wei Woo Department of Physics Northwestern University Evanston, Illinois 60201	1
Dr. Robert M. Hexter Department of Chemistry University of Minnesota Minneapolis, Minnesota 55455	1
Dr. R. P. Van Duyne Chemistry Department Northwestern University Evanston, Illinois 60201	1
Dr. S. Sibener Department of Chemistry James Franck Institute 5640 Ellis Avenue Chicago, Illinois 60637	1
Dr. M. G. Lagally Department of Metallurgical and Mining Engineering University of Wisconsin Madison, Wisconsin 53706	1

TECHNICAL REPORT DISTRIBUTION LIST, 056

	No. Copies		No. Copies
Dr. Robert Gomer Department of Chemistry James Franck Institute 5640 Ellis Avenue Chicago, Illinois 60637	1	Dr. K. G. Spears Chemistry Department Northwestern University Evanston, Illinois 60201	1
Dr. R. G. Wallis Department of Physics University of California, Irvine Irvine, California 92664	1	Dr. R. W. Plummer University of Pennsylvania Department of Physics Philadelphia, Pennsylvania 19104	1
Dr. D. Ramaker Chemistry Department George Washington University Washington, D.C. 20052	1	Dr. E. Yeager Department of Chemistry Case Western Reserve University Cleveland, Ohio 41106	1
Dr. P. Hansma Physics Department University of California, Santa Barbara Santa Barbara, California 93106	1	Professor D. Hercules University of Pittsburgh Chemistry Department Pittsburgh, Pennsylvania 15260	1
Dr. J. C. Hemminger Chemistry Department University of California, Irvine Irvine, California 92717	1	Professor N. Winograd The Pennsylvania State University Department of Chemistry University Park, Pennsylvania 16802	1
Dr. Martin Fleischmann Department of Chemistry Southampton University Southampton SO9 5NH Hampshire, England	1	~~Professor T. F. George~~ ~~The University of Rochester~~ ~~Chemistry Department~~ ~~Rochester, New York 14627~~	1
Dr. G. Rubloff IBM Thomas J. Watson Research Center P. O. Box 218 Yorktown Heights, New York 10598	1	Professor Dudley R. Herschbach Harvard College Office for Research Contracts 1350 Massachusetts Avenue Cambridge, Massachusetts 02138	1
Dr. J. A. Gardner Department of Physics Oregon State University Corvallis, Oregon 97331	1	Professor Horia Metiu University of California, Santa Barbara Chemistry Department Santa Barbara, California 93106	1
Dr. G. D. Stein Mechanical Engineering Department Northwestern University Evanston, Illinois 60201	1	Professor A. Steckl Rensselaer Polytechnic Institute Department of Electrical and Systems Engineering Integrated Circuits Laboratories Troy, New York 12181	1

TECHNICAL REPORT DISTRIBUTION LIST, 056

	No. Copies	No. Copie
Dr. John T. Yates Department of Chemistry University of Pittsburgh Pittsburgh, Pennsylvania 15260	1	
Professor G. H. Morrison Department of Chemistry Cornell University Ithaca, New York 14853	1	
Captain Lee Myers AFOSR/NC Bolling AFB Washington, D.C. 20332	1	
Dr. David Squire Army Research Office P. O. Box 12211 Research Triangle Park, NC 27709	1	
Professor Ronald Hoffman Department of Chemistry Cornell University Ithaca, New York 14853	1	

END

FILMED

7-83

DTIC